Soft Matter

Destruction of cancer cells by laser-induced shock waves: recent developments in experimental treatments and multi scale computer simulations

Journal:	*Soft Matter*
Manuscript ID:	SM-EMA-02-2014-000407.R1
Article Type:	Emerging Area
Date Submitted by the Author:	31-Mar-2014
Complete List of Authors:	Steinhauser, Martin; Fraunhofer Ernst-Mach-Institut, Research Group Shock Waves in Soft Biological Matter; University of Basel, Faculty of Science, Chemistry Department Schmidt, Mischa; Fraunhofer Ernst-Mach-Institut, Research Group Shock Waves in Soft Biological Matter

ARTICLE TYPE www. rsc.org/xxxxxx | XXXXXXXX

Destruction of cancer cells by laser-induced shock waves: recent developments in experimental treatments and multiscale computer simulations

Martin Oliver Steinhauser,[*a,b] and Mischa Schmidt[a]

Received Xth XXXXXXXXXX 20XX, Accepted Xth XXXXXXXXX 20XX
First published on the web Xth XXXXXXXXXX 200X
DOI: 10.1039/b000000x

In this emerging area article we review recent progress in the mechanical destruction of cancer cells using laser-induced shock waves. The pure mechanical damaging and destruction of cancer cells associated with this technique possibly opens a new route to tumor treatments and corresponding therapies. At the same time progress in multiscale simulation techniques makes it possible to simulate mechanical properties of soft biological matter such as membranes, cytoskeletal networks and even whole cells and tissue. In this way an interdisciplinary approach to understanding key mechanisms in shock wave interactions with biological matter has become accessible. Mechanical properties of biological materials are also critical for many physiological processes and cover length scales ranging from the atomistic to macroscopic scale. We argue that latest developments and progress in experimentation enable the investigation of shock wave interaction with cancer cells on multiple time- and length-scales. In this way the integrated use of experiment and simulation can address key challenges in this field. The exploration of the biological effects of laser-generated shock waves on a fundamental level constitutes an emerging multidisciplinary research combining scientific methods from the areas of physics, biology, medicine and computer science.

1 Introduction

Cancer is not only one single disease but occurs in many different pathologic conditions that widely differ in terms of molecular biology, clinical course and prognosis. However, common to all cancer types is the occurrence of malignant neoplasia showing uncontrolled proliferation as well as invasion of adjacent tissues and metastasis, mainly through the lymph or blood system.[1] Recent experimental results indicate that during malignant transformation of cells changes in their cytoskeleton and plasma membrane occur which lead to significant changes in the mechanical properties of neoplasia, which in turn is a prerequisite for all three pathomechanisms of malignancy.[2–4] Hence, biomechanical changes, i.e. changes in the cytoskeleton or the plasma membrane are fundamental processes and even help for the diagnosis of cancer.[5–8] Consequently, the targeted mechanical destruction of parts of the membrane or the cytoskeleton of tumor cells might prevent neoplasia from metastasing through the body or even lead to cell death.

Traditionally, the only cure for cancer has been surgery, i.e. resection of solid tumor tissue.[9] Open surgery however is always associated with a high risk for the patient, suppression of a patient's immune system and a significant mortality and morbidity rate. Minimally invasive techniques as an alternative to open surgery for localized tumor treatment, such as radiofrequency ablation,[10–13] cryoablation[14–16] or direct laser ablation[17,18] are methods which use a range of energies for direct *in situ* tumor destruction through energy absorption and killing by heating or evaporation. Connected with this treatment are several unwanted side-effects such as killing of healthy tissue, long duration of treatment or cutaneous burns which delimits acceptance of these methods among patients.

Besides direct conversion of mechanical energy into heat, biological material may be damaged by the effects of mechanical stress caused by shock waves.[19] Such effects can be caused for example by cavitation induced shockwaves which can occur in ultrasound treatments. It has been shown that shock waves interacting with cells within small enough time intervals (on the order of nanoseconds) do not lead to any significant increase of temperature.[20]

An efficient way to generate shock waves in biological systems became available to biomedical research by the use of high-power lasers shortly after the invention of the Q-switched pulsed laser in the 1960s.[21] Short laser pulses can generate stress waves by either optical breakdown in water or air,[22,23]

[a] *Fraunhofer Research Group "Shock Waves in Soft Biological Matter", Ernst-Mach-Institut, EMI, Eckerstrasse 4, Freiburg, Germany. Fax: +49 761 2714-1424; Tel: +49 761 2714-424; E-mail: martin.steinhauser@emi.fraunhofer.de*
[b] *Department of Chemistry, Faculty of Science, University of Basel, Klingelbergstrasse 80, CH-4056 Basel, Switzerland*

ablation of a target material,[24,25] or rapid heating and expansion of an absorbing medium.[26,27] Laser-induced optical breakdown in water or air occurs when the laser pulse energy per volume in the medium is high enough to generate a plasma in a spatially confined region. Associated with plasma formation are physical processes such as shock wave generation and cavitation. The spatial extend of the laser-induced breakdown effects can be reduced by lowering the incident laser-pulse energy. However, there is a lower limit to the pulse energy since a threshold intensity is necessary to initiate the breakdown process. In the decades succeeding the introduction of the laser in clinical and basic research, the generation and properties of laser-induced shock waves (LISW) and the role of mechanical effects in the interaction of LISW with biological cells and tissue became the subject of intense research.[28–35]

The development of extracorporeal shock wave lithotripsy (ESWL) in the 1980s provided yet another tool for the generation of shock waves which evolved as a clinical standard, widely used as the only non-invasive surgical technique to eliminate kidney stones and other urinary calculi.[36] ESWL uses focused high-amplitude pressure waves that are generated in a contact medium outside the patient's body by a piezoelectric, electrohydraulic or electromagnetic transducer, called lithotripter. The patient is positioned in such a way that the stone is in the focus of the pressure wave. When the acoustic energy deposited in the focal region is high enough, cavitation bubbles filled with vapor or gas form and collapse violently. This collapse results in formation of a shock wave that in turn contributes to disintegrating the stone. The multiple mechanisms associated with stone disintegration by ESWL as well as current advances in instrumentation and clinical praxis are described elaborately by Rassweiler.[34] Apart from stone destruction, ESWL can cause tissue injury as unwanted adverse effects during treatment. Consequently, the study of interaction effects of stress waves with biological tissue and cells has become a recurrent topic in shock wave research.[27,30,37–39]

With the given experimental progress and the fast ongoing developments both in computer hardware and multiscale modelling strategies of soft biological systems in computational science, we are today in a position to study the fundamental effects of the interaction of shock waves with biological soft matter not only on the mere macroscopic experimental scale but also on the cellular and even sub-cellular level. With computational coarse-graining techniques which subsume some of the atomistic degrees of freedom by introducing new particles comprising many hundreds or thousands of atoms, much larger length and time scales can be reached in molecular simulations than is possible with pure atomistic or even quantum chemical methods.[40–44] Coarse-grained models for simulating biological structures which are part of a cell, such as phospholipid bilayers and the cytoskeleton involving many millions of particles, have offered to use molecular dynamics simulations for the investigation of the mechanical destructive effects of shock waves in complex biomolecules.[45] In this way computational methods can underpin and support shock wave experiments of biological systems in a way which would not have been feasible ten years ago.

In this paper, we intend to highlight recent progress in the experimental investigation of laser-induced shock wave effects on cells, along with several exciting recent developments in applications of multiscale modeling and simulation to explore the interaction of shock waves with soft biological matter. Experimental progress with techniques such as photon Doppler velocimetry (PDV) and the use of high-precision hydrophones allow for a very precise characterization of shock wave profiles.[46] New possible shock wave applications such as drug delivery and gene therapy have emerged[33,47,48] and new multiscale methods for modeling and simulating biological systems have been developed in computational science during the last decade.[42,49–51] We argue that with these new experimental and computational developments we are seeing a new emerging research area that focuses on exploring the interaction of shock waves with tumor cells and the possible destructive and therapeutic effects. A thorough understanding of these effects might as well lead to the introduction of laser-induced shock wave treatment as a new, additional form of tumor therapy.

2 The impact of shock waves on cells

Both, LISW and lithotripter induced shock waves are broadband, unipolar waves. However, LISW do not produce a measurable tensile component, see Fig. 1 and thus exclude all biological effects induced by cavitation which are very hard to control experimentally.[36,52] Cavitation is caused by the tensile part of a shock wave and pressure measurements, e.g. with hydrophones in this context are done relative to the (hydrostatic) pressure before shock wave impact. Hence, a negative pressure, as can be seen in Fig. 1 describes a tensile wave. Also, the rise times of shock waves generated with lithotripters differ remarkably from less than 30 *ns* to over 600 *ns*. This, along with the necessity to use many shock pulses to generate significant biological effects, causes studies based on lithotripter generated shock waves to be comparable to each other only to limited extent.

Therefore, LISW are a better tool to systematically study biological effects of shock waves than ESWL, because they eliminate all other known sources of cellular injury such as cavitation, thermal denaturation, formation of free radicals and bulk displacement. Thus, an experimental examination of the cellular response to the pure mechanical stress effects is possible. The characteristics of LISW depend on the laser parameters wavelength, pulse duration and pulse energy, but

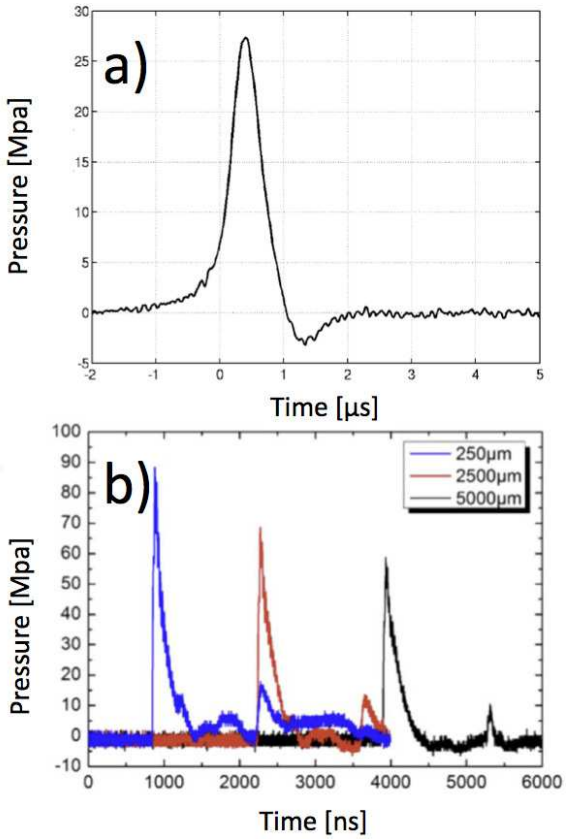

Fig. 1 a) A typical pressure recording of of a lithotripter shock wave passage. Note the drop of pressure to -3 *MPa* after 1 μs. Due to the limited rise time of the hydrophone used, the rise time of the pressure amplitude is underestimated.[53] b) Typical shock wave signals of a laser-induced shock wave displaying no tensile part. The pressure profiles shown were recorded with high-precision hydrophones at positions $z = 250\,\mu m$ (blue), $z = 2500\,\mu m$ (red) and $z = 5000\,\mu m$ (black), where z is the distance between the location of shock wave generation and the hydrophone probe tip.[54]

also on the mechanical and optical properties of the target material.[32]

2.1 Shock wave induced cell permeability and drug delivery

As reviewed by Yao, LISW are able to render the cell membrane permeable, allowing for drug delivery and gene transfection.[55] The application to whole tissue structures is also possible. For example, transdermal insulin delivery by LISW results in a reduction of the blood glucose level without causing any pain to the patient.[56]

With lithotripter shock waves it is also possible to permeabilize cells without killing them by reducing the deposited energy below the lethal value.[29,47,57–60] In this way, molecules present in the surrounding medium can diffuse into the cells.[61] In several recent studies, adherently grown cells on transparent substrates were exposed to shock waves and analyzed with (fluorescence-) microscopy. In direct vicinity of cavitation bubbles, the cells are completely destroyed and detached from the surface.[53,62] Cells close to the bubbles are permanently permeabilized and killed, whereas cells further away from the bubbles survive. This behavior can be attributed to deformations of the cytoskeleton.[63] The fact that ESWL can cause tissue damage, inspired experiments that applied lithotriper induced shock waves to tumors *in vivo*. While several first studies in animal models did not show any impact of shock waves on tumor growth,[64] some results seemed encouraging, for example a delayed tumor growth in mice[65] and even complete remission of dorsal skin tumors in hamsters.[66]

Parallel to the *in vivo* experiments on tumors, a large number of *in vitro* studies on different cell lines in culture were performed as reviewed by Coleman[64] and Delius.[67] Most striking for a possible shock wave based tumor therapy was a study on different normal and malignant cell lines, which showed no selective effect.[38]

Up to date, shock wave treatment based on ESWL has not been used in clinical traits. This is probably because the physical mechanisms related to the cavitation phenomenon that cause both stone destruction and tissue damage are complex, not well understood, hardly experimentally controllable, and because no selective effects on cells have been observed.[38,67]

2.2 Laser-induced mechanical shock waves

When irradiating an absorbing material with a pulsed laser, the optical energy deposited on the absorber is transformed into mechanical energy. A shock wave forms at the surface and then propagates through the absorber.[68] The shock wave properties such as rise time, velocity of propagation or peak pressure depend on the absorbing material and the laser parameters. For one specific laser/absorber system, the peak stress of the shock wave can be tuned by varying the laser fluence that is equal to the total energy deposited per area of illumination.[25,69,70] In this experimental configuration, well-defined, reproducible shock waves can be generated without the side effect of heating or cavitation.[39] Thus, the pure mechanical effect of the shock wave on the cells can be investigated.

Figure 2 shows the basic features of the experimental setups used in several initial studies performed by Doukas and others.[28,29,71–74] The laser beam is directed onto the bottom of a cell culture vessel, that consists of an absorbing material. Upon illumination with the laser, a shock wave is formed that travels into the vessel, and interacts with the cells. For beam diameters of a few millimeters, peak pressures up to approximately 100 *MPa* can be obtained.

In many early studies of the 1980s to 1990s, the effects

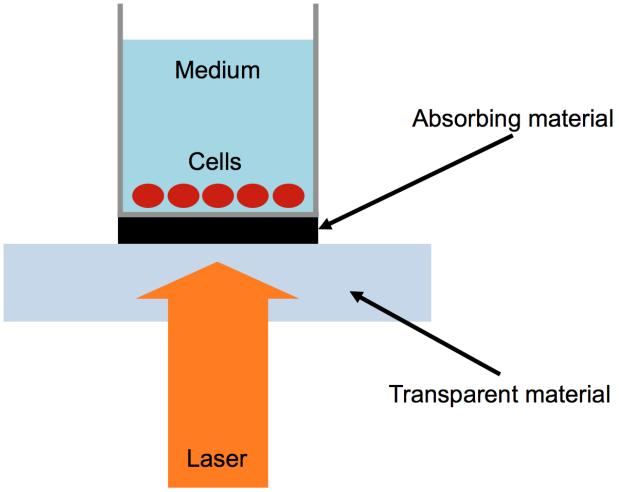

Fig. 2 Basic elements of the experimental setups used to study the effects of laser induced shock waves on cells.[28,29,71–74] A pulsed laser beam irradiates an absorbing material at the bottom of the vessel that contains the cells and their growth medium. At the surface of the absorber, a shock wave is formed that moves forward into the vessel. When the absorbing material is covered with a transparent material facing the laser, the peak pressure of the shock wave is further enhanced.[70]

caused by shock waves could not always be clearly separated from those caused by direct laser irradiation or probable contamination of cell cultures which were used as *in vitro* models. In addition, a precise characterisation of the shock wave profile was very often not done due to a lack of precision of hydrophone measurements, and proper control experiments were not always performed or reported. The repetitive use of the same polymer (usually polyimide) as target material for shock wave generation, can – as we know today – diversify the resulting profile of shock waves due to changing absorbance of the polymer even after the first laser pulse.[75,76] In experimental setups of early studies, the polyimide film often formed one end of a narrow pipette tube in direct contact with the target cells, which decreased the reproducibility of the experiments.[29,71] Thus, studies of the biological effects of shock waves induced by pulsed laser ablation of polymer films have generally been hindered by difficulties in reproducible growth conditions of cell cultures and by the difficulty of generating well-characterized and reproducible pressure pulses whose temporal and spatial characteristics are known. For future applications in the medical sciences it is essential to study not only single cells but more complex systems such as tissues. In this context, as the biological soft matter under investigation is more complex, its physical properties have to be very well characterized and be reproducible. This is one of the challenges for future studies in the field.

In one of the early studies of the 1990s it was concluded that for one specific cell line the survival rates of cells exposed to LISW depend on the stress gradient $\sigma = p_{\max}/\tau_r$, where $p_{\max}$ is the peak pressure and τ_r is the rise time of the shock wave.[71] The rise times of the shock waves in this study were varied between 10 and 30 *ns*. However, repetitive laser shots (5 times) were used which renders the results of these experiments less reproducible and reliable. In fact, the survival rates among different cell lines differ remarkably at constant physical parameters $(p_{\max}, \tau_r)$. For example, only 50% of transformed (immortalized) retinal pigment epithelium cells survive exposure to shock waves with $p_{\max} = 74\ MPa$ and $\tau_r = 10\ ns$. However, 100% of normal retinal pigment epithelium cells survive this procedure.[74] A shock wave with $\tau_r = 10\ ns$ and $p_{\max} = 30\ MPa$ kills 50% of mouse breast sarcoma cells,[71] whereas human promelocytic leukemia cells survive this exposure.[29]

All of the above mentioned studies that use the experimental principle denoted in Fig. 2 have had major disadvantages in the techniques used to characterize the physical conditions in the vessel containing the medium with the cells. Also, in many of these studies reproducible cell culture preparation was problematic, introducing many possible sources of errors into the experiment. For example, in some studies the cells were treated with gel and ice (but some were not), or only cell suspensions instead of real adherently grown monolayers were used, thus reducing the reproducibility of the experiments. The pressure profiles are measured with piezoelectric elements (Polyvinylidene fluoride, PVDF) either in form of needle hydrophones or piezoelectric films that are brought in contact to the surface of the culture vessel. In both cases, a transfer medium (either water or grease) serves as the acoustic contact to the piezoelectric element. However, shock waves are known to decay rapidly (within micrometers) in liquids and tissue.[77–79] Thus, the need for a fluid as contact medium may lead to wrong pressure measurements and it would be desirable to determine shock wave properties on a microscopic scale, rather than on a much coarser scale with a PVDF sensor of millimeter dimensions.

A newly developed optical method to determine the pressure profiles is photon Doppler velocimetry.[46] This technique has very recently been used in a comprehensive study to determine the velocity profile of the bottom of the vessel during shock wave propagation. The measured profiles served as input for molecular dynamics simulations that compute the pressure fields within the whole vessel with high time resolution. In this way, the local pressure conditions, i.e. the pressure levels directly at the location of the cells during the shock wave experiment could be thoroughly characterized. Furthermore, the pressure threshold for the destruction of human brain tumor cells (U87 glioblastoma) could be determined.[54]

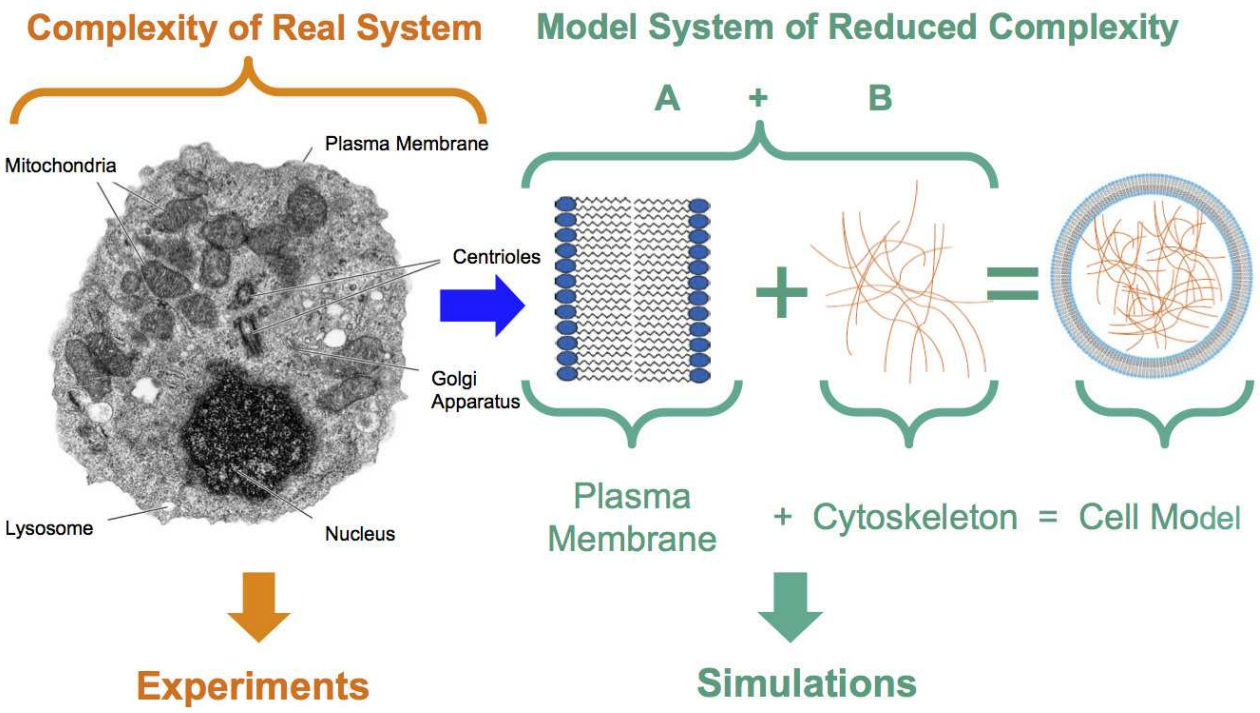

Fig. 3 An integrated approach combining the full complexity of the real experimental system with computational coarse-grained (CG) models of reduced complexity. In CG models, typically, only two major components of cells determining their mechanical properties relevant for their interaction with shock waves are considered.

3 Multiscale modeling approaches in cancer research

Multiscale approaches for computational modeling of mechanical properties of biological materials has developed into an emerging area of research. The key to understanding complex diseases like cancer is to have a systematic comprehension of the relevant processes at the cellular, sub-cellular and molecular level. Progress in biomolecular modeling and computational method development can give additional insight to this end and a whole range of simulation and modeling methods have been developed.[80–83] When it comes to the effects of mechanical destruction or damage of cancer cells induced by shock waves, it is a useful approach to reduce the complexity of the problem by focusing on the two major components of an eucariotic cell which are responsible for most of its mechanical properties: the plasma membrane and the cytoskeleton, see Fig. 3.

Perhaps the most obvious challenge in simulating the properties of biological macromolecules is their large size, impaired by the necessity to include at least a representative part of their environment. This includes the surrounding solvent, proteins or cofactors which may be bound to a protein or membrane. The area of biomolecular modelling is still evolving, and it is not yet at a stage where exact, quantitative predictions of, for example, binding or free energies, ligand bindings or other dynamical features of sub-cellular structures can be routinely made. Therefore, it is very important to link simulation approaches with experimental observations.

Traditionally, computational biology has been mostly an adoption of atomistic or ab-initio molecular dynamics or Monte-Carlo methods from chemistry and physics, often used as a black box tool to complement experimental large-scale research efforts in genomics, glycomics, proteomics, structure-aided drug design and structural biology. Thus, strong skepticism of any computational modeling results is sometimes encountered among experimentalists even today and is just as misguided as blind acceptance of numerical results without critical analysis. Here, it is crucial for the computational scientist to clarify the assets and limitations of current computational approaches. For example, biomolecular all-atom simulations are still limited to the nanosecond regime and to a few thousand atoms.[42]

The integrated use of computational and experimental methods at multiple scales provides a powerful approach to elucidate key mechanisms in the effects of laser-induced shock waves when interacting with tumor cells and neoplasia. In the following we focus first on coarse-grained mechanical models

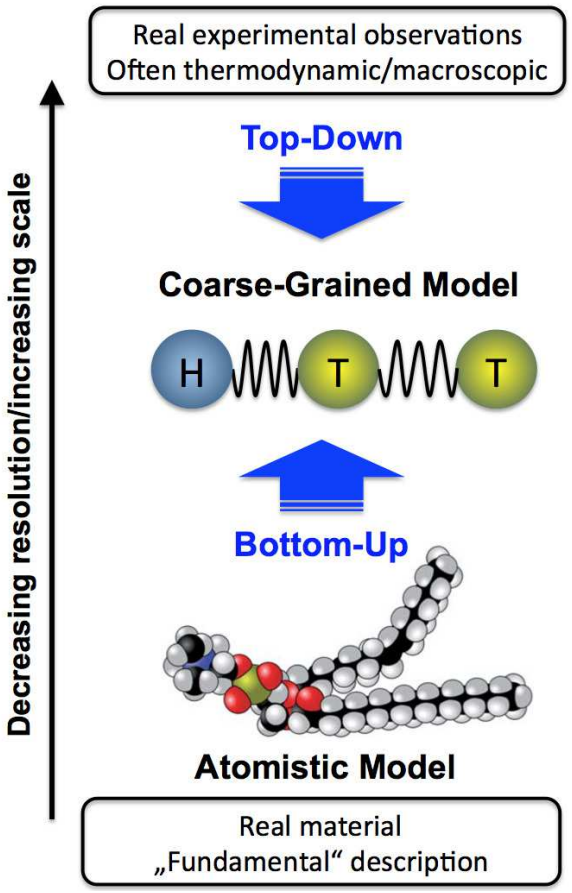

Fig. 4 Scheme illustrating top-down and bottom-up strategies for developing CG computational models for a common phospholipid molecule (DPPC, dipalmitoylphosphatidylcholine, $C_{40}H_{80}NO_8P$) most frequently occurring in plasma membranes.[45] The CG model is a typical bead-spring model of polymer physics composed of three parts, one hydrophilic head (H) particle and two hydrophobic tail (T) particles, connected by bonds that are described by entropic springs.[40,42]

for bilayer membranes and cytoskeleton networks. We then turn toward latest computational developments that combine these approaches with the numerical study of mechanical effects of shock waves in these complex structures which has created a new research area.

3.1 Coarse-grained models of membrane dynamics

Coarse-grained (CG) models provide a route to explore biomolecular systems on longer time and length scales.[42,84] They constitute a class of mesoscale model, in which many atoms are treated by grouping them together into new particles which act as individual interaction sites usually connected by entropic springs, see Fig. 4.

CG models were introduced originally for globular proteins by Levitt and Warshel in a pioneering 1970s paper[85] (then called hybrid classical/quantum mechanical approach) and since then have found their way into polymer physics as so-called bead-spring models,[40] as well as into engineering, geophysics and other areas of computational research.

A "bottom-up" CG model is a model of a particular system that is constructed on the basis of a more detailed model for the same system as indicated in Fig. 4. In principle, the high-resolution, all-atom model may be based on atomistic data deduced from atomistic structure calculations.

In contrast, "top-down" models do not rely upon or directly relate to a more detailed model for a particular system. Instead, they are usually related to the full complexity of the real experimental system by addressing observables on length scales that are accessible to the CG model. Often, these observables are thermodynamic averaged quantities such as pressure, temperature, stress and strains or forces accessible by direct experimental measurement. Figure 4 illustrates schematically these two major approaches to coarse-graining.

CG simulations are much less computationally expensive than their atomistic counterparts, because the number of interacting particles is drastically reduced and can access much larger length- and time scales than is possible in all-atom approaches, let alone in quantum chemical calculations.[86–88] Coarse graining procedures may simply remove certain degrees of freedom (e.g. vibrational modes between two atoms) or it may in fact simplify the two atoms completely via a single particle representation. The ends to which systems may be coarse grained is simply bound by the accuracy in the dynamics and structural properties one wishes to replicate. The challenge of this modern area of research is still in its infancy, and although it is commonly used in biological modeling and polymer physics, the analytic theory behind it is still poorly understood.

There is a very large body of literature on computational studies of the static and dynamic properties of biomembranes using atomistic and CG modelling approaches[89,90] which have been reviewed in depth e.g. by Pandit and Scott[91] and Woods and Mulholland.[88]

With the rise of so-called *solvent-free*, or *implicit* simulation schemes for membranes, which became fashionable at the turn of the millennium, the number of publications in this field has constantly increased. Solvent-free models of lipid bilayer structures do not explicitly take the fluid molecules of the aqueous environment into account. These models are either based on a Langevin equation of motion accounting for the Brownian random motion of the fluid molecules, or on the complete modeling of all effects of the solvent by effective interaction potentials between the constituent particles of the membrane only.[92–95] As one is usually only interested in the structural and dynamic details of the membrane and not in the

surrounding fluid, this allows to reduce the number of necessary integrations and thus the computational costs considerably. Many of the used potentials are either derived from intuition, from standard potentials routinely being using in polymer physics or from quantum chemical calculations of force field parameterizations.[81,89,96,97]

Almost all of the existing simulation studies of biomembrane properties have been performed at or very near at equilibrium. When it comes to studying the shock wave interaction with biomembrane structures, which is a highly transient and non-equilibrium process, there is only a handful of papers, all of them limited to very small all-atom simulations with explicitly modeled solvent and not taking into account the particular thermodynamic transient conditions of shock waves.[98–100]

In a very recent research paper that provided a new multiscale approach to this problem, it was discussed that even in the largest of these all-atom simulations published to date, the size of the considered system was several orders of magnitude too small in size and too limited in the time scale to be able to capture any relevant effects of shock waves in membranes observed in experiments such as transient permeability and subsequent self-repair of parts of the membrane in an eucariotic cell.[101]

3.2 Coarse-grained polymer network models of the cytoskeleton

An important part of the eucariotic cell is its cytoskeleton. The cytoskeleton is a network of semi-flexible and rod-like macromolecules which is responsible for providing structural integrity, mechanical stability and for protecting the cells' constituents from external forces.[102] It also plays various roles of much higher complexity. Through self-organization, the cytoskeleton can even exert forces on its surroundings, which enables the cell to perform locomotion and change its shape. It is therefore responsible for the cell's motility and migration abilities.

In particular with cancer cells' mechanical changes in the stiffness of the cytoskeleton by alterations in genetic expression, a bottom-up approach in computational modeling has been proven essential since the microstructure of reconstituted systems can be systematically controlled in the modeling process.[106]

The cytoskeleton mainly consists of three types of long, filamentous proteins: F-actin, intermediate filaments and microtubules. They all differ in their roles, structure and size. Actin microfilaments for example are about 6-8*nm* wide, intermediate filaments 10*nm*, and microtubules are hollow with 14*nm* inner and 25*nm* outer diameter.

The three filament types diversely contribute to the mechanical stability of the cytoskeleton and the cell, since they differ quite drastically in their own stiffness. While microtubules

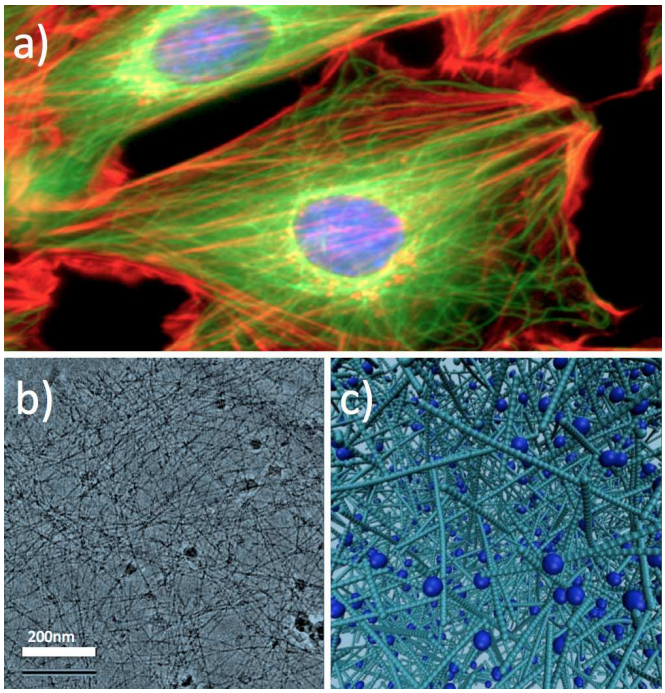

Fig. 5 a) A mouse NIH3T3 fibroblast cell, fixed and stained for DNA (blue) and the major cytoskeletal filaments actin (red) and alpha-tubulin (green). The cell was imaged by fluorescence microscopy on an optical IX70 microscope with a deep-cooled CCD camera.[103] b) Image of the actin cytoskeleton (lamellipodium) showing a relatively sparse network in a frozen hydrated sample.[104] c) Computed network structure of the cytoskeleton based on molecular dynamics simulations of semi-flexible polymers including cross linking particles.[105]

mainly resist compression, actin and intermediate filaments help maintaining the cell-shape by bearing tension. The bending stiffness of a filament can be characterized with help of the worm-like chain model and the persistence length L_p, concepts which are introduced in polymer physics.[107] For example, the flexural rigidity of microtubules corresponds to a persistence length of $5,200$ microns showing that a microtubule is rigid even over cellular dimensions. By contrast, the persistence length of an actin filament is only approximately 17.7 microns, explaining why actin filaments within cells are usually cross-linked into bundles. The filaments are called "intermediate", because, in the smooth muscle cells where they were first discovered, their diameter (about $10\,nm$) is between that of the thin actin-containing filaments and the thicker myosin filaments. Intermediate filaments are the toughest and most durable of the three cytoskeletal filaments: when cells are treated with non-ionic detergents and concentrated salt solutions, the intermediate filaments survive while most of the rest of the cytoskeleton is destroyed. Intermediate filaments typically form a network throughout the cytoplasm, sur-

rounding the nucleus and extending out to the cell periphery. They are often anchored to the plasma membrane at cell-cell junctions, called desmosomes, which helps to resist shearing forces and large strain deformation. This appears to be especially relevant for resisting the large stresses caused by laser-induced shock waves.

Many of the mechanical properties of the cytoskeleton are attributed to the biopolymer actin.[108] Above the overlap concentration actin filaments form entangled solutions that are mechanically weak. The elasticity of such a solution can be considerably enhanced by actin binding proteins which act as crosslinkers and depends on their effect on the network microstructure and their micro-mechanical and biochemical properties.

Semiflexibility and stiffness can be introduced in CG models of polymer networks by appropriate potentials.[109] Computer simulations of network models of the cytoskeleton of eucariotic cells are usually based on CG approaches of entangled polymer networks as they have been commonly used in polymer physics for decades.[110] Figure 5 shows two examples of the morphology of actin and tubulin networks along with a CG model based on a molecular dynamics approach.[104,105] The whole host of literature available in macromolecular atomistic and CG network models has been reviewed comprehensively by Mofrad and Kamm.[111]

With the increase of computing power it has now become feasible to combine the hitherto separate investigations of networks and biomembranes to a combined approach in an attempt to create simple mechanical models of cells that mimic some of the key elastic-viscoelastic properties of real cellular systems and even tissue.[80,112]

3.3 Combining shock wave research with coarse-grained simulations

The exploration of shock wave effects, bond breaking and failure with CG models of soft biological systems coined an important emerging field of research which has been introduced only a few years ago.[45,113,114] This new approach combines coarse-graining with coupling the atomistic and the continuum domain. The surrounding aqueous environment which is only needed to transfer the energy of a shock wave to the mechanical model of a membrane, is coarse-grained using continuum theory. At the same time, those areas of interest within the membrane where dynamic damage or failure occurs, can still be modeled with either atomistic resolution, or by using a further CG description of molecular structures, see Fig. 6.

Full atomistic simulations are not capable of capturing the time- and length-scales important for understanding key effects when a shock wave hits a lipid bilayer membrane and induces potential damage to the cytoskeleton. By combining latest results in modeling and multiscale simulation techniques

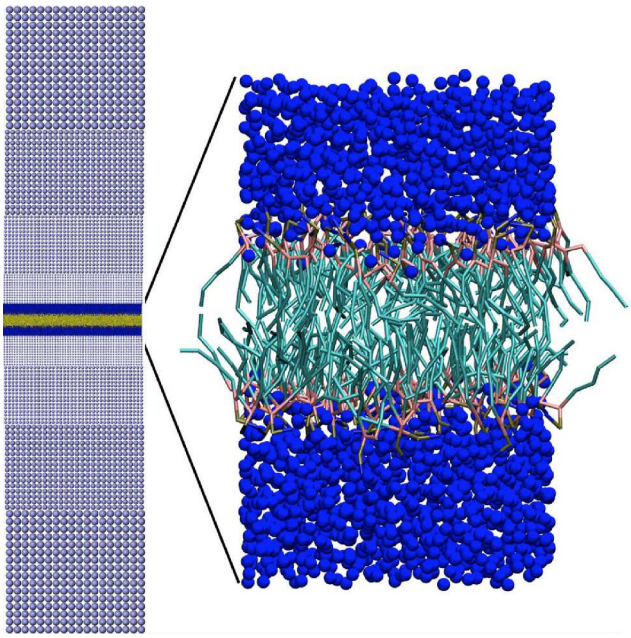

Fig. 6 Multiscale model of a membrane including atomistic details in the regime of the phospholipids and a multi-resolution continuum model in the fluid regime based on a simulation technique called smooth particle hydrodynamics (SPH).[101]

it has even become possible to perform impact simulations which incorporate the salient mechanical features of a cell, the cytoskeleton with its semi-flexibility, the plasma membrane with its bending rigidity, the fluid environment within the cell, and the aqueous surrounding of the cell, cf. Fig. 7.

4 Summary and future directions

This article has given a brief account of recent experimental and computational developments in the application of shock wave research to cancer treatment which constitutes an emerging research area with numerous exciting perspectives. Significant progress in this field can only be made with multidisciplinary approaches, including biomedical molecular modeling, computational chemistry, biophysics and the medical sciences. Simulation efforts can contribute on all levels of biological complexity to a better understanding of complex diseases like cancer. Thus, rather than focusing on very accurate studies on the finest level including only a few atoms and extremely small systems, new methodological developments are needed on all levels such as CG, mesoscale and macroscale models. An integration of all these tools could allow a multiresolution view on various aspects of relevant biological processes occurring in the shock wave interaction with whole cancer cells, tumor tissue and even on the organic scale.

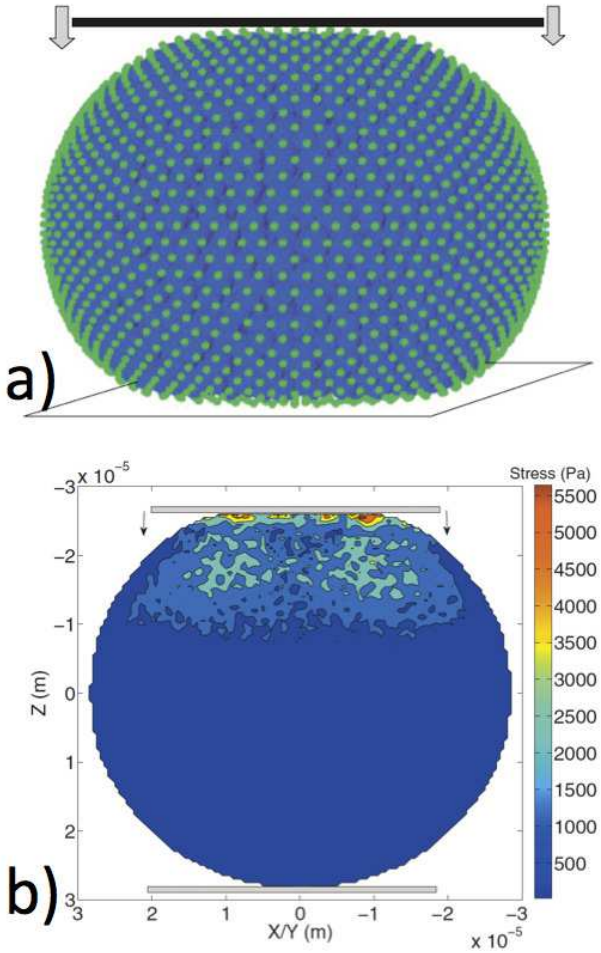

Fig. 7 a) Snapshot of a simulated particle-based cell model, impacted with a plate with velocity $v = 5ms^{-1}$. b) Simulated protoplasmic effective shear stresses developing at at time of impact, as a function of the projected position in the x, y, z plane of the cell. [115]

References

1 G. I. Evan and K. H. Vousden, *Nature*, 2011, **411**, 342–348.

2 R. A. Weinberg, *The Biology of Cancer*, Garland Science, 1st edn., 2007.

3 C. Ainsworth, *Nature*, 2008, **456**, 696–699.

4 E. Jonietz, *Nature*, 2012, **491**, S56–S57.

5 S. M. S. Hurtley, *Science*, 1998, **279**, 459.

6 P. Friedl and K. Wolf, *Nature Rev. Cancer*, 2003, **3**, 362–374.

7 X. Trepat, L. Deng, S. S. An, D. Navajas, D. J. Tschumperlin, W. T. Gerthoffer, J. P. Butler and J. J. Fredberg, *Nature*, 2007, **447**, 592–595.

8 D. A. Fletcher and R. D. Mullins, *Nature*, 2010, **463**, 485–492.

9 B. B. Dunn, *Nature*, 2011, **483**, S2–S6.

10 L. Eisenberg, A. Mauro, W. W. L. Glenn and J. H. Hageman, *Science*, 1968, **147**, 578–582.

11 D. J. Ott, *Am. J. Gastroenterol.*, 2003, **98**, 2564–2565.

12 L. Lackey, C. Peterson and R. G. Barr, *Ultrasound Quarterly*, 2012, **28**, 269–274.

13 T. G. Simona, M. D. Belanda, J. T. Machanb, T. DiPetrilloc and D. E. Dupuya, *Eur. J. Radiol.*, 2012, **81**, 4167–4172.

14 T. K. Sotsky and T. S. Ravikumar, *Semin. Oncol.*, 2002, **29**, 183–191.

15 D. B. Johnson and S. Y. Nakada, *J. Endourol.*, 2003, **17**, 627–632.

16 J. Goyal, P. Verma, A. Sidana, C. S. Georgiades and R. Rodriguez, *J. Endourol.*, 2012, **26**, 1413–1419.

17 T. J. Vogl, R. Straub, K. Eichler, O. Söllner and M. G. Mack, *Radiology*, 2004, **230**, 450–458.

18 M. Nikfarjam and C. Christophi, *Br. J. Surg.*, 2003, **90**, 1033–1047.

19 F. Suhr, Y. Delhasse, G. Bungartz, A. Schmidt, K. Pfannkuche and W. Bloch, *Stem Cell Res.*, 2013, **11**, 951–964.

20 L. D. Johns, *J. Athl. Train.*, 2003, **37**, 239–299.

21 E. F. Carome, N. A. Clark and C. E. Moeller, *Appl. Phys. Lett.*, 1964, **4**, 95–97.

22 B. Zysset, J. G. Fujimoto, C. A. Puliafito, R. Birngruber and T. F. Deutsch, *Lasers Surg. Med.*, 1989, **9**, 193–204.

23 A. Vogel and W. Lauterborn, *J. Acoust. Soc. Am.*, 1988, **84**, 719–731.

24 R. Srinivasan, *Science*, 1986, **234**, 559–565.

25 V. Venugopalan and T. F. Deutsch, *J. Appl. Phys.*, 1993, **74**, 4181–4189.

26 B. Sullivan and A. C. Tam, *J. Acoust. Soc. Am.*, 1984, **75**, 437–441.

27 A. Sondén, B. Svensson, N. Roman, H. Ostmark, B. Brismar, J. Palmblad and B. T. Kjellström, *Lasers Surg. Med.*, 1999, **26**, 364–375.

28 S. Lee and A. G. Doukas, *IEEE J. Sel. Top. Quant.*, 1999, **5**, 997–1003.

29 T. Kodama, M. R. Hamblin and A. G. Doukas, *Biophys. J.*, 2000, **79**, 1821–1832.

30 A. Sondén, B. Svensson, N. Roman, B. Brismar, J. Palmblad and B. T. Kjellstöm, *Lasers Surg. Med.*, 2002, **31**, 233–241.

31 A. V. Cherian and K. R. Rau, *J. Biomed. Opt.*, 2008, **13**, 024009.

32 C. Yao, X. Qu, Z. Zhang, G. Hüttmann and R. Rahmanzadeh, *J. Biomed. Opt.*, 2009, **14**, 054034-1 – 05403-7.

33 P. Chakravarty, W. Qian, M. A. El-Sayed and M. R. Prausnitz, *Nat. Nanotechnol.*, 2010, **5**, 607–611.

34 J. J. Rassweiler, T. Knoll, K.-U. K. ohrmann, J. A. McAteer, J. E. Lingeman, R. D. Cleveland, M. R. Bailey and C. Chaussy, *Eur. Urol.*, 2011, **59**, 784–796.

35 H. W. Baac, J. Frampton, J. G. Ok, S. Takayama and L. J. Guo, *J. Biophotonics*, 2013, **6**, 905–910.

36 J. E. Lingeman, J. A. McAteer, E. Gnessin and A. P. Evan, *Nat. Rev. Urol.*, 2009, **6**, 660–670.

37 N. Fischer, H. M. Muller, A. Gulhan, M. Sohn, F. J. Deutz, H. Rubben and W. Lutzeyer, *J. Endourol.*, 1988, **2**, 215–220.

38 F. Brümmer, T. Bräuner and D. F. Hülser, *World J. Urol.*, 1990, **8**, 224–232.

39 A. G. Doukas and T. J. Flotte, *Ultrasound Med. Biol.*, 1995, **22**, 151–164.

40 M. O. Steinhauser, *Recent Res. Devel. Physics*, 2006, **7**, 26–59.

41 T. A. Knotts, N. Rathore, D. C. Schwartz and J. J. de Pablo, *J. Chem. Phys.*, 2007, **126**, 084901-1 – 084901-12.

42 M. O. Steinhauser, *Computational Multiscale Modeling of Fluids and Solids: Theory and Applications*, Springer, Heidelberg, Berlin, New York, 1st edn., 2008.

43 H. A. Karimi-Varzaneh and F. Müller-Plathe, *Top. Curr. Chem.*, 2011, **307**, 295–321.

44 M. O. Steinhauser, in *Molecular Dynamics-Studies of Synthetic and Biological Macromolecules.(InTech Open Science, 2012)*, ed. L. Wang, Introduction to Molecular Dynamics Simulations: Applications in Hard and Soft Condensed Matter Physics, 2012, pp. 3-28.

45 G. C. Ganzenmüller, S. Hiermaier and M. O. Steinhauser, *Soft Matter*, 2011, **7**, 4307–4317.

46 O. T. Strand, D. R. Goosman, C. Martinez, T. L. Whitworth and W. W. Kuhlow, *Rev. Sci. Instrum.*, 2006, **77**, 083108-1 – 083108-8.

47 U. Lauer, E. Bürgelt, Z. Squire, K. Messmer, P. H. Hofschneider, M. Gregor and M. Delius, *Gene. Ther.*, 1997, **4**, 710–715.

48 M. R. Prausnitz and R. Langer, *Nat. Biotechnol.*, 2008, **26**, 1261–1268.

49 P. Sherwood, B. R. Brooks and M. S. P. Sansom, *Curr. Opin. Struct. Biol.*, 2008, **18**, 630–640.

50 M. J. Buehler, *J. Mech. Behav. Biomed.*, 2010, **4**, 125–127.

51 P. Causin, R. Sacco and M. Verri, *Biomech. Model Mechan.*, 2013, **12**, 763–780.

52 C. C. Coussios and R. A. Roy, *Annu. Rev. Fluid Mech.*, 2008, **40**, 395–420.

53 C.-D. Ohl and B. Wolfrum, *Biochim. Biophys. Acta*, 2003, **1624**, 131–138.

54 M. Schmidt, U. Kahlert, J. Wessolleck, D. Maciaczyk, B. Merkt, J. Maciaczyk, J. Osterholz, G. Nikkhah and M. O. Steinhauser, *Sci. Rep.*, 2014, **4**, 3849.

55 C.-P. Yao, Z.-X. Zhang, R. Rahmanzadeh and G. Huettmann, *IEEE Trans. Nanobiosci.*, 2008, **7**, 111–119.

56 A. G. Doukas and N. Kollias, *Adv. Drug Deliver Rev.*, 2004, **56**, 559–579.

57 S. Bao, B. D. Thrall, R. A. Gies and D. L. Miller, *Cancer Res.*, 1998, **58**, 219–221.

58 M. Delius and G. Adams, *Cancer Res.*, 1999, **59**, 5227–5232.

59 G. Hartmann, R. Jox, S. Thompson, A. Eigler, A. Krug, S. Erhardt, S. Endres, M. Delius, K. Tschoep and G. Adams, *J. Molec. Med.*, 2001, **79**, 306–313.

60 T. Kodama, A. G. Doukas and M. R. Hamblin, *Cancer Lett.*, 2003, **189**, 69–75.

61 M. S. Michel, P. Erben, L. Trojan, A. Schaaf, K. Miknavelidze, T. Knoll and P. Alken, *Anticancer Res.*, 2004, **24**, 2303–2308.

62 C.-D. Ohl, M. Arora, R. Ikink, N. de Jong, M. Versluis, M. Delius and D. Lohse, *Biophys. J.*, 2006, **91**, 4285–4295.

63 S. F. Moosavi-Nejad, S. M. R. Hosseini, M. Satoh and K. Takayama, *Cancer Sci.*, 2006, **97**, 296–304.

64 A. J. Coleman and J. E. Saunders, *Ultrasonics*, 1993, **31**, 75–89.

65 G. O. Oosterhof, G. A. Smits, A. E. De Ruyter, J. A. Schalken and F. M. Debruyne, *Ultrasound Med. Biol.*, 1990, **17**, 391–399.

66 F. Gamarra, F. Spelsberg, M. Dellian and A. E. Goetz, *Int. J. Cancer*, 1993, **55**, 153–156.

67 M. Delius, *Shock Waves*, 1994, **4**, 55–72.

68 J. C. Bushnell and D. J. McCloskey, *J. Appl. Phys.*, 1968, **39**, 5541–5546.

69 L. C. Yang, *J. Appl. Phys.*, 1974, **45**, 2601–2608.

70 R. Fabbro, J. Fournier, P. Ballard, D. Devaux and J. Virmont, *J. Appl. Phys.*, 1990, **68**, 775–784.

71 A. G. Doukas, D. J. McAuliffe, S. Lee, V. Venugopalan and T. J. Flotte, *Ultrasound Med. Biol.*, 1995, **21**, 961–967.

72 S. Lee, T. Anderson, H. Zhang, T. J. Flotte and A. G. Doukas, *Ultrasound Med. Biol.*, 1996, **22**, 1285–1293.

73 S. E. Mulholland, S. Lee, D. J. McAuliffe and A. G. Doukas, *Pharm. Res.*, 1999, **16**, 514–518.

74 T. Douki, S. Lee, K. Dorey, T. J. Flotte, T. F. Deutsch and A. G. Doukas, *Lasers Surg. Med.*, 1996, **19**, 249–259.

75 T. Lippert, M. Hauer, C. R. Phipps and A. Wokaun, *Appl. Phys. A*, 2003, **77**, 259–264.

76 H. Y. Yoshikawa, J. Cui, K. Kratz, T. Matsuzaki, S. Nakabayashi, A. Marx, U. Engel, A. Lendlein and M. Tanaka, *J. Phys. Chem. B*, 2012, **116**, 8024–8030.

77 T. Juhasz, X. H. Hu, L. Turi and Z. Bor, *Lasers Surg. Med.*, 1993, **15**, 91–98.

78 T. Juhasz, G. A. Kastis, C. Suárez, Z. Bor and W. E. Bron, *Lasers Surg. Med.*, 1995, **19**, 23–31.

79 A. Vogel, S. Busch and U. Parlitz, *J. Acoust. Soc. Am.*, 1996, **100**, 148–165.

80 C. T. Lim, E. H. Zhou and S. T. Quek, *J. Biomech.*, 2006, **39**, 195–216.

81 S. W. I. Siu, R. Vácha, P. Jungwirth and R. A. Böckmann, *J. Chem. Phys.*, 2008, **128**, 125103-1 – 125103-12.

82 M. W. van der Kamp, K. E. Shaw, C. J. Woods and A. J. Mulholland, *J. R. Soc. Interface*, 2008, **5 Suppl 3**, S173–S190.

83 T. Schlick, R. Collepardo-Guevara, L. A. Halvorsen, S. Jung and X. Xiao, *Quarterly Rev. Biophys.*, 2011, **44**, 191–228.

84 M. O. Steinhauser, *J. Chem. Phys.*, 2005, **122**, 094901-1 – 094901-13.

85 A. Warshel and M. Levitt, *J. Molec. Biol.*, 1976, **103**, 227–249.

86 L. R. Forrest and M. S. Sansom, *Curr. Opin. Struct. Biol.*, 2000, **10**, 174–181.

87 S. O. Nielsen, C. F. Lopez, G. Srinivas and M. L. Klein, *J. Phys.: Condens. Matter*, 2004, **16**, R481–R512.

88 C. J. Woods and A. J. Mulholland, *Chem. Modell.*, 2008, **5**, 13–50.

89 R. Chang, G. S. Ayton and G. A. Voth, *J. Chem. Phys.*, 2005, **122**, 244716-1–244716-12.

90 M.-J. Huang, R. Kapral, A. S. Mikhailov and H.-Y. Chen, *J. Chem. Phys.*, 2012, **137**, 055101-1–055101-10.

91 S. A. Pandit and H. L. Scott, *Biochim. Biophys. Acta*, 2009, **1788**, 136–148.

92 O. Farago, *J. Chem. Phys.*, 2003, **119**, 596-605.

93 G. Brannigan, P. F. Philips and F. L. H. Brown, *Phys. Rev. E*, 2005, **72**, 011915-1–011915-4.

94 H. Yuan, C. Huang, J. Li, G. Lykotrafitis and S. Zhang, *Phys. Rev. E*, 2010, **82**, 011905-1–011905-8.

95 H. Noguchi, *J. Chem. Phys.*, 2011, **134**, 055101-1–055101-12.

96 S. J. Weiner, P. A. Kollman, D. A. Case, U. C. Singh, C. Ghio, G. Alagona, S. Profeta and P. Weiner, *J. Am. Chem. Soc.*, 1984, **106**, 765–784.

97 W. Paul, D. Y. Yoon and G. D. Smith, *J. Chem. Phys.*, 1995, **103**, 1702-1709.

98 K. Koshiyama, T. Kodama, T. Yano and S. Fujikawa, *Biophys. J.*, 2006, **91**, 2198–2205.

99 K. K. Koshiyama, T. T. Kodama, T. T. Yano and S. S. Fujikawa, *Biochim. Biophys. Acta*, 2008, **1778**, 1423–1428.

100 J. Lechuga, D. Drikakis and S. Pal, *Int. J. Numer. Meth. Fl.*, 2008, **57**, 677–692.

101 G. C. Ganzenmüller, S. Hiermaier and M. O. Steinhauser, *PLoS ONE*, 2011, **7**, e51989.

102 O. Lieleg, K. M. Schmoller, C. J. Cyron, Y. Luan, W. A. Wall and A. R. Bausch, *Soft Matter*, 2009, **5**, 1796–1803.

103 S. Suresh, *Acta Biomater.*, 2007, **3**, 413–438.

104 G. P. Resch, K. N. Goldie, A. Krebs, A. Hoenger and J. V. Small, *J. Cell Sci.*, 2002, **115**, 1877–1882.

105 R. D. Kamm, Bulletin of the American Physical Society, 2006, p. 30.

106 A. R. Bausch and K. Kroy, *Nat. Phys.*, 2006, **2**, 231–238.

107 M. O. Steinhauser, *Mech. Time-Depend. Mater.*, 2008, **12**, 291–312.

108 M. G. Saunders and G. A. Voth, *Structure*, 2012, **20**, 641–653.

109 M. O. Steinhauser, J. Schneider and A. Blumen, *J. Chem. Phys.*, 2009, **130**, 164902-1–164902-8.

110 K. E. Evans and S. F. Edwards, *J. Chem. Soc., Faraday Trans. 2*, 1981, **77**, 1891-1912.

111 M. Mofrad and R. D. Kamm, *Cytoskeletal Mechanics: Models and Measurements in Cell Mechanics*, Cambridge University Press, 2006.

112 P. Ghysels, G. Samaey, B. Tijskens, P. van Liedekerke, H. Ramon and D. Roose, *Phys. Biol.*, 2008, **6**, 016009.

113 G. C. Ganzenmüller, S. Hiermaier and M. O. Steinhauser, *Eur. Phys. J. Spec. Top.*, 2012, **206**, 51–60.

114 M. O. Steinhauser, AES Technical Reviews, Part C, IJATEMA, Ottawa, 2012, pp. 15–29.

115 P. van Liedekerke, E. Tijskens, H. Ramon, P. Ghysels, G. Samaey and D. Roose, *Phys. Rev. E*, 2010, **81**, 061906-1 – 061906-15.

Complexity of Real System

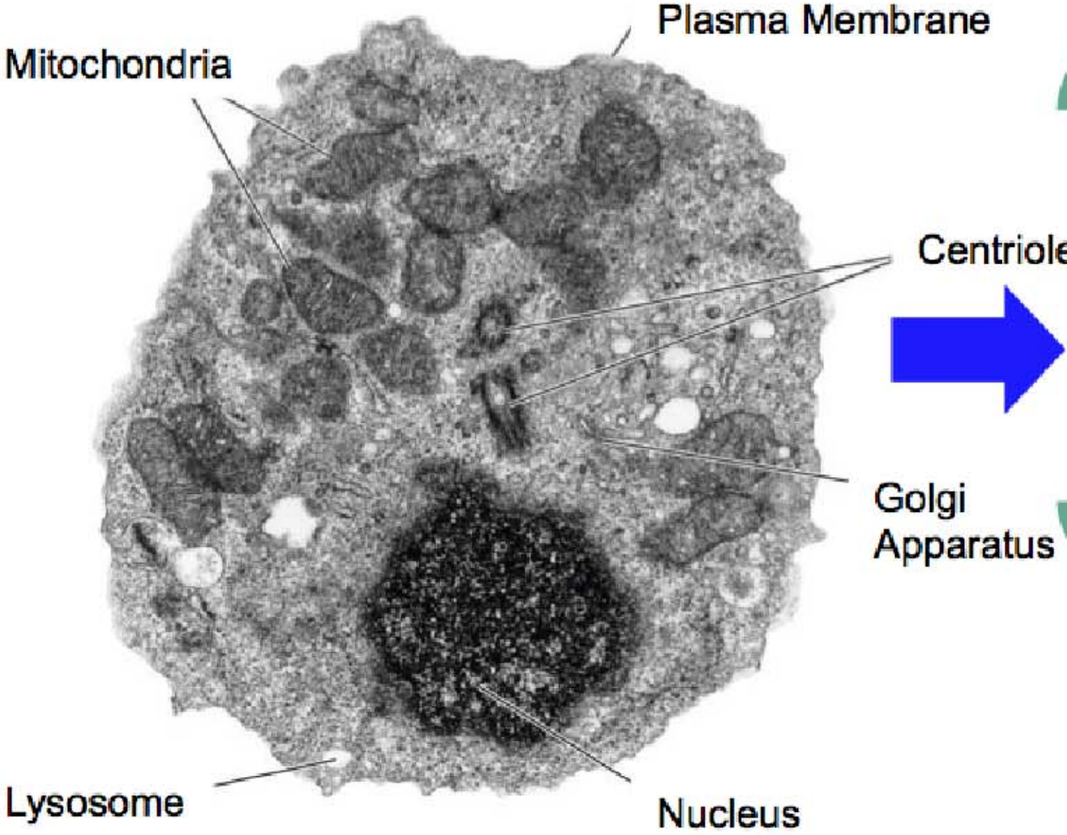

Model System of Reduced Complexity

A + B

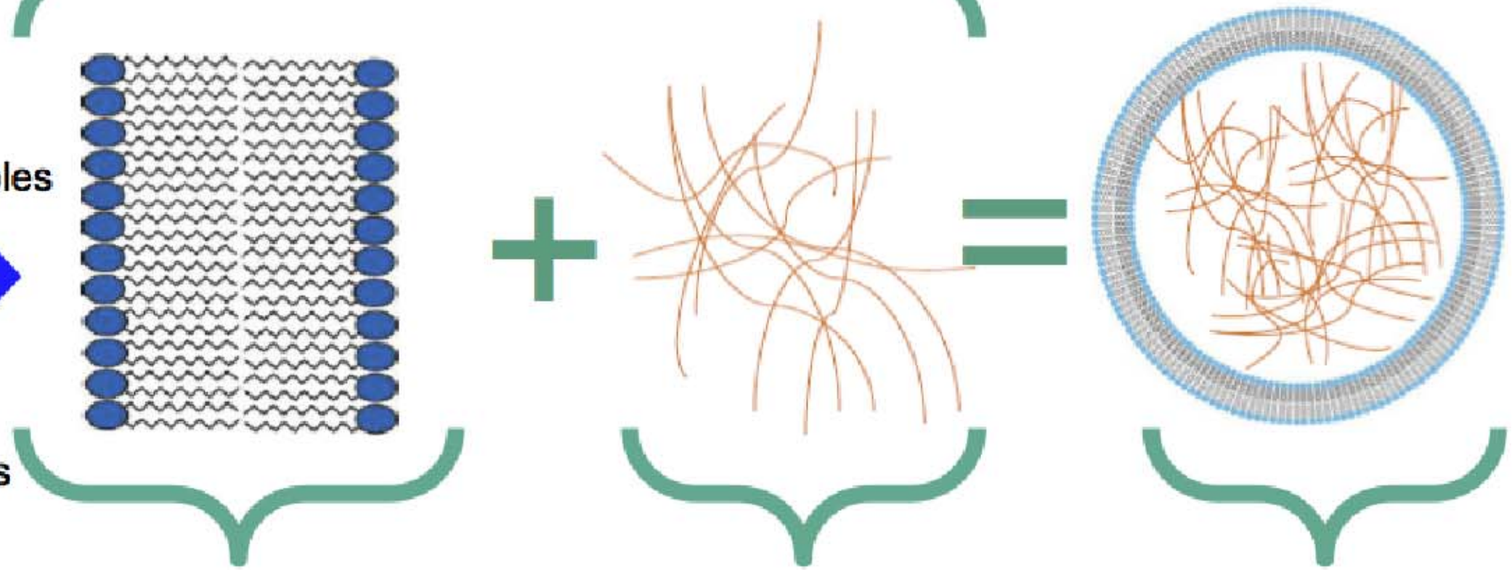

Plasma Membrane + Cytoskeleton = Cell Model

Experiments

Simulations